

The effects of a third element on structure and properties of W–C/N

M.T. Vieira*, A. Cavaleiro, B. Trindade

ICEMS, Grupo de Materiais e Engenharia de Superfícies, Departamento de Engenharia Mecânica, Pólo II, Universidade de Coimbra, Pinhal de Marrocos, 3030 Coimbra, Portugal

Abstract

In order to improve the mechanical and thermal properties of hard coatings to be used in cutting tools, the addition of a third element to the carbides and nitrides of transition metals is nowadays current practice [J. Mater. Sci. 32 (1997) 4463]. However, the stability of the new structures due to the presence of a third element is one of the most important problems to overcome. We have studied the effect of adding different metallic (Fe, Co, Pd, Cr, Ti, Ni,...) and non-metallic (Si) elements to the structure of W–C/N-based films deposited by sputtering. The influence of a Group VIII element on interstitial carbides has also been studied in order to clarify its role in structure amorphization. The results obtained for films in the as-deposited condition show different types of structures with various degrees of structural order, depending on the type and content of the element added. The new coatings can be structurally stable or metastable, formed either by structures with enlarged solubility domains or amorphous structures, with or without nanophases inside. The transformation kinetics of the metastable phases with temperature for different types and contents of a third element added have been investigated. From the results obtained at high temperatures, we conclude that the chemical and structural behavior mainly depends on the position of the third element in the Periodic Table, and on its affinity to carbon and nitrogen. Strong and moderate carbide/nitride-forming elements improve the phase stability at high temperatures; the other elements lead to structural changes in the operating temperature range of the coating during the technological application. © 2002 Elsevier Science B.V. All rights reserved.

Keywords: Tungsten carbide; Tungsten nitride; W–C/N–M; W–N–Si; Interstitial phases; Hard coatings

1. Introduction

Tungsten carbide with metallic binders, such as cobalt, is still one of the most common bulk materials used in applications requiring high hardness at high temperatures [1,2], good wear resistance (abrasion and erosion) and high corrosion resistance, particularly in acidic media. Cermets based on tungsten carbide are commonly used in severe conditions of cutting and drilling of hard alloys, rocks, wood particleboard, etc. However, due to their low dissociation energy and toughness, they are not suitable for some cutting conditions. Modification of the chemical composition, morphology and structure by the rapid deposition of tungsten and non-metallic light-element thin films on hard substrates (such as cemented carbide or high-speed steels) contributes to improvement of the cutting performance of the tools. Some authors claim that materials based on tungsten–

non-metallic light elements alloyed with metals can be used as coatings for high-speed steels, or even cemented carbides [3–16].

With regard to the physical vapor deposition of W-based systems, most of the work published refers to either non-reactive sputtering from WC [7,12] or WC–M (M=transition metal) [17–28] targets, or deposition in a reactive atmosphere (enriched in carbon or nitrogen) from W (one [5,29] or two targets [30]), W–C [5] or W–C–M (M=transition metal) [31,32] targets.

This paper is a review of our work so far and provides a step towards better understanding of the interaction among chemical composition, structure, thermal stability and mechanical properties of tungsten–carbon/nitrogen sputtered thin films alloyed with a third element (weaker or stronger forming carbides/nitrides). It aims to draw attention to the importance of the interaction of carbon or nitrogen and the third element in the formation of better performing and stable structures of W–C/N-based materials. The results obtained for W-based systems are extrapolated to other interstitial phases on the

* Corresponding author. Tel.: +351-39-790700; fax: +351-39-790701.

E-mail address: teresa.vieira@mail.dem.uc.pt (M.T. Vieira).

Table 1
Limits of third element concentrations in sputtered W-based thin films

Element content of W–M–C/N system (at.%)	Co	Ni	Fe	Cr	Au	Pd	Ti	Si
C < 30	–	0–14	–	–	–	–	0–50	–
30 < C < 80	0–22	0–24	0–31	0–21	0–32	0–33	0–34	–
N < 39	–	0–15	–	–	–	–	0–33	0–50
39 < N < 60	–	–	–	–	–	–	0–36	0–50

basis of experimental data on the role of third element in other M–C carbides (M = Ti, V, Mo,...).

2. Experimental details

2.1. Sample preparation

One set of the W-based thin films was produced by sputtering of sintered W, W + M or Si (M = Co, Fe, Ni, Ti, Pd, Au) targets with M or Si contents from 4 up to 50 at.% in a reactive atmosphere enriched in carbon or nitrogen. The other set consisted of films prepared from W–C and W–N and (WC) + M targets by non-reactive sputtering. In the last case, a cemented tungsten carbide sputtering target was partially covered with thin foils of metallic elements. By varying the ratio between the exposed area of the base material target and the area of the thin foil composed of the third element, the content of the third element in the films was changed. The reactive deposition of W–Si–N was performed from a W target encrusted with a varying number of Si slices. The silicon content in the films was changed in the same way as in the case of the thin metal foils. In order to validate the study for other carbides and nitrides of transition metals, the films of M–M_i–C (where M ≠ M_i, and M_i = Group VIIIA of the Periodic Table) were sputtered from composite targets of sintered M_xC_y placed upon M_i plates. In all cases, the substrate was heat-treated high-speed steel with hardness of 8.5–9.0 GPa. The substrates were polished with diamond paste with a particle size down to 3 μm, resulting in a surface roughness of R_a = 0.025–0.030 μm. Prior to deposition, the substrates were cleaned in situ by ion bombardment in an argon plasma. The sputter deposition parameters are described in detail elsewhere [7,19–21,24–32]. The thickness of the thin films prepared was measured using a surface profilometer, giving a result of approximately 3 μm.

A study of the effect of metallic and non-metallic elements on the thermal stability of W-based thin films was performed by isochronal annealing of the coated samples at temperatures of up to 1000 °C in vacuum ($P = 10^{-4}$ Pa). Concomitantly, differential scanning calorimetry (DSC) measurements were carried out on films detached from the substrates within the temperature

range 20–1200 °C at a continuous rate of 20 °C/min in an Ar + H₂ or N₂ + H₂ atmosphere.

2.2. Film characterization

Chemical and structural analysis of the as-deposited and heat-treated films was performed by means of electron probe microanalysis (EPMA; Cameca SX50), X-ray diffraction (XRD; X'Pert Philips diffractometer) and transmission electron microscopy (TEM; Jeol 200 CX microscope). XRD measurements using CoK_α radiation were performed in both conventional θ –2 θ mode (Bragg–Brentano geometry) and glancing angle (4° incident angle) modes. Morphological characterization of the samples was performed using a scanning electron microscope (SEM; Jeol T330). The hardness of the coatings was measured using ultra-microhardness equipment (Fisherscope H100) equipped with a Vickers indenter. Loads of 50, 100, 200, 300, 500 and 1000 mN were applied, and the load vs. indentation depth was continuously monitored.

3. Results and discussion

3.1. Chemical composition

The chemical composition of as-deposited films ranged between the limits shown in Table 1. In order to point out the role of the third element, pure W–C and W–N systems were deposited as standards. The N and C fractions were assumed to have values of 0–60 and 0–80 at.%, respectively. The carbon or nitrogen content was changed either by the chemical composition of the targets or by the partial pressure of C or N in the chamber atmosphere during deposition. The content of the third element in the films was a function of the target chemical composition and/or substrate bias, and varied from 0 to 50 at.%. The tungsten carbide thin films deposited from WC targets, with or without the addition of a third element, were always deficient in carbon. In the majority of W–M–C systems, carbon deficit in the films decreases with increasing M content, with the exception being the films with gold, where the higher the gold content is, the higher is the carbon deficit [38].

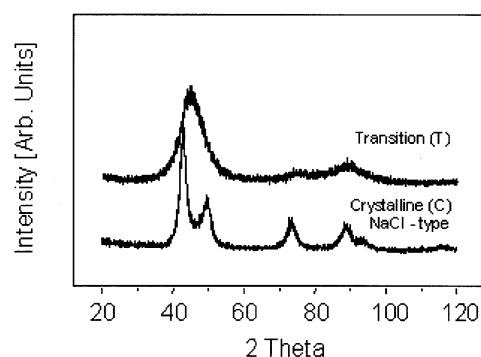


Fig. 1. Type I X-ray diffractograms: (a) crystalline NaCl-type (bottom); (b) nanocrystalline (top).

3.2. Film structure

Representative XRD patterns of the W-based films are presented in Figs. 1 and 2. Depending on the chemical composition of the film, three types of structure are observed

- Type I: crystalline, composed of solid solutions and/or carbides or nitrides of tungsten;
- Type II: amorphous; and
- Type III: amorphous with nanocrystalline phases.

Type I can assume two different aspects, depending on the chemical composition. The first corresponds to diffractograms with relatively sharp peaks, in spite of the solute content and intrinsic stresses due to the sputtering process. The second structure is characteristic of uncompleted crystallization of the material, with relatively broad peaks, and such a structure has higher M content than the previous one.

The type II XRD patterns are characteristic of amorphous materials, with a broad main peak and weaker sub-peaks. These were obtained from films with a low content of nitrogen, carbon or metal admixture. The value required for the M content for film amorphization depends on the element's position in the Periodic Table, and increases from right (Ni) to left and from bottom

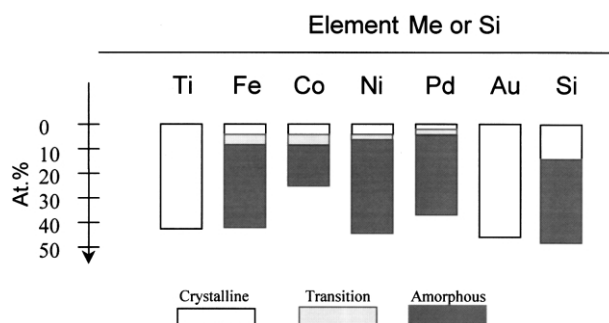


Fig. 3. The role of the third element in the formation of an amorphous phase.

to top. Therefore, the difference in atomic radius between tungsten and the third element can also play an important role, as is the case for gold or titanium, where the similar atomic radii constrain any changes in the structure. In accordance with the XRD results, the TEM analysis of crystalline structures reveals a fine-grained phase. For elements other than gold or titanium, the increase in M content, whatever the level of carbon or nitrogen in the coating, leads to an amorphous structure, characterized by a type II diffractogram and fairly contrasted TEM images, associated with diffuse and broad electron diffraction (ED) rings (Fig. 2). Fig. 3 summarizes the effects of the third metal element on the structure of the as-deposited W-based thin film.

In the phases with a low content of metal admixture, the metal atom can substitute W in the b.c.c. α -W lattice — the phase that occurs in films with low C or N content. The small quantities of the metal element contribute to dilatation of the lattice [33]. In coatings with high carbon and nitrogen contents the β -WC_{1-x} carbide and β -W₂N nitride phases occurred. However, in the case of nitride, the indexed structure does not correspond to the nitrogen content in the film (55 at.%), indicating that some unbonded nitrogen should be pres-

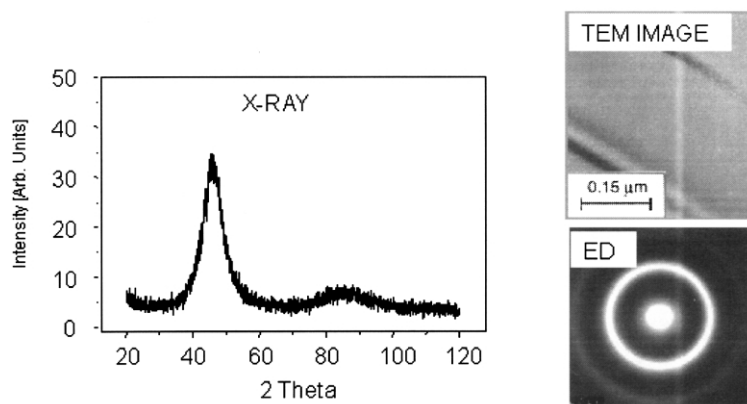


Fig. 2. X-Ray diffractogram, TEM bright-field image and electron diffraction of the amorphous phase in W₄₈Co₁₁C₄₁ thin films.

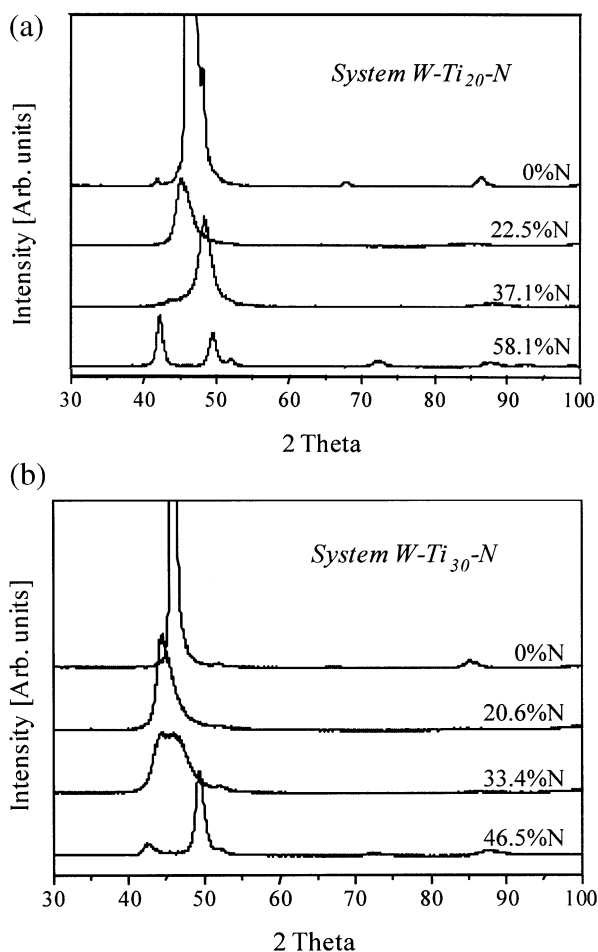


Fig. 4. The effects of nitrogen content on the interplanar distances of $W-Ti_{20}-N$ and $W-Ti_{30}-N$.

ent in the nitride matrix. In $W-Si-N$ films, the $\beta-W_2N$ phase is also present at high fractions of Si and N.

The increase in nitrogen content in $W-M-C/N$ films, with $M=Ti$, leads to an increase in the $\alpha-W$ lattice constant (Fig. 4); for higher fractions of carbon and nitrogen, the presence of the metallic third element contributes to the formation of crystalline phases in the $W-M-C/N$ films, with $M=Ti$, Cr or Au, which are composed of a fine-grained crystalline f.c.c. structure of $\beta-MC_{1-x}$ ($M=W, M$), or by NaCl-type f.c.c. isomorphous phases: $\beta-W_2N$ and/or TiN and $\alpha-W$ for higher values of Ti in $W-Ti-N$ systems. The diffractograms of high titanium-content films have an asymmetric line, which allowed the identification of two diffraction peaks after deconvolution: one was indexed as $\alpha-W$ (low 2θ values), whereas the other (main peak) was attributed to the lattice plane (200) of $\beta-W_2N$ and/or TiN (Fig. 5).

However, the films with M =metal of Group VIIIA become progressively amorphous with increasing M content, even for low values of the interstitial element; the crystalline \rightarrow amorphous structural transition occurs

for M concentrations in the range 5–13 at.% [34]. The crystalline $W-(Fe, Co, Ni, Pd)-C/N$ films are composed of a fine-grained NaCl-type f.c.c. structure, similar to $W-M-C/N$ ($M=Ti, Cr, Au$) films. The addition of an element from Group VIII to $W-C/N$ results in the occurrence of an amorphous structure, regardless of the non-metallic element content. The spatial arrangement of the amorphous $W-C/N$ -based systems is not completely random and maintains some degree of short-range order. It was shown elsewhere [38] that such films could be regarded as an atomically heterogeneous mixture composed of regions of very small crystallites of $\beta-MC_{1-x}$ or $\beta-M_2N$ rich in W , and regions of an amorphous phase rich in element M .

The $W-Si-N$ films with high nitrogen and silicon content exhibit predominantly amorphous structures (type II). For films with low nitrogen content, it is possible to observe the X-ray lines of b.c.c. $\alpha-W$ superimposed on a broad amorphous diffraction peak (type III) (Fig. 6). The crystalline phase has very small grains, from 15 down to 3 nm in size. For the W/Si atomic ratio examined for the films deposited, amorphicity should be expected [34–36]. Nevertheless, Ger Vanishvili and Munir [37] suggest the possibility of obtaining WSi_2 in materials with low Si content.

The amorphization in $W-C/N$ -based films can be attributed to different causes: the distortion of the carbide or nitride lattice due to the difference between the atomic radius of tungsten and the third element, and the different affinity of the latter for carbon or nitrogen compared to that of tungsten. Although gold and palladium have a similar atomic radius, they exhibit a different effect regarding the amorphization of $W-C/N$ films. It is obvious that other factors are involved, such as the substitution of W with an element, which weakens the $W-C$ chemical bonding and strengthens the W -metal bonding, resulting in growth of the amorphous phase. On the contrary, the addition of a stronger

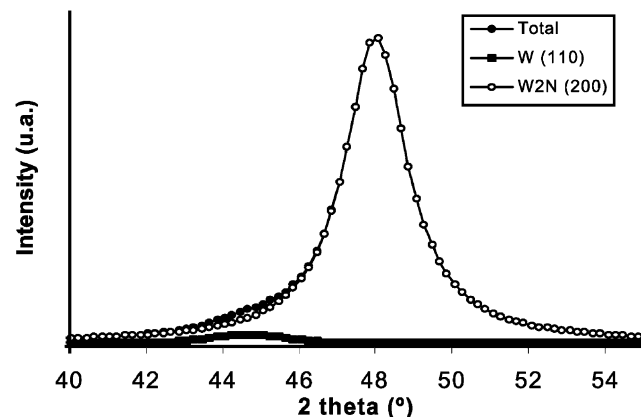


Fig. 5. Deconvolution of the main diffraction peak of the $W-Ti-N$ sputtered film.

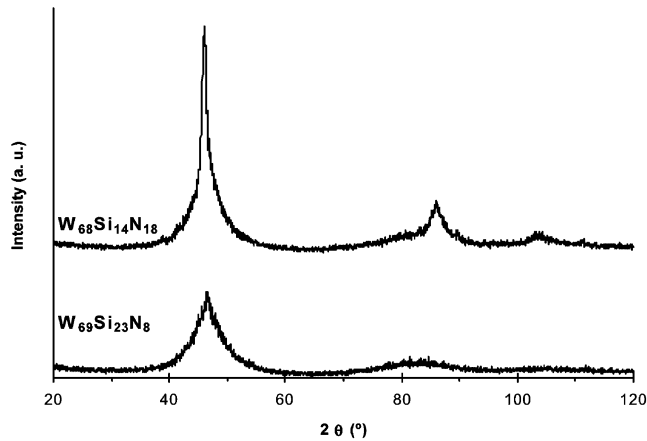


Fig. 6. X-Ray diffractograms of a mixed nanocrystalline and amorphous phase in W–Si–(low N) thin films.

carbide- or nitride-forming element should give rise to a crystalline structure, whatever the element content. This is clearly shown in the case when M is titanium, where even 50 at.% is not enough to cause amorphization. Furthermore, a low addition of titanium to amorphous films is sufficient to obtain crystalline films [27]. However, the addition of silicon, which has a strong affinity for carbon and nitrogen, gives rise to an amorphous phase if its content in the thin film is higher than 15 at.%. Such behavior is probably due to the huge difference between the radius of W and Si, perhaps inducing a new interstitial phase.

The ternary diagrams shown in Fig. 7 summarize the structure of sputtered thin films as a function of W, Me/Si and C/N atomic contents.

The effect observed for a third element in W–C/N thin films may be extrapolated to other transition metal carbides/nitrides. In order to extend the results obtained for W-based hard coatings, experiments with a third element from Group VIII of the Periodic Table admixed in carbides of other transition metals were performed. Fig. 8 summarizes the structural evolution of the M–

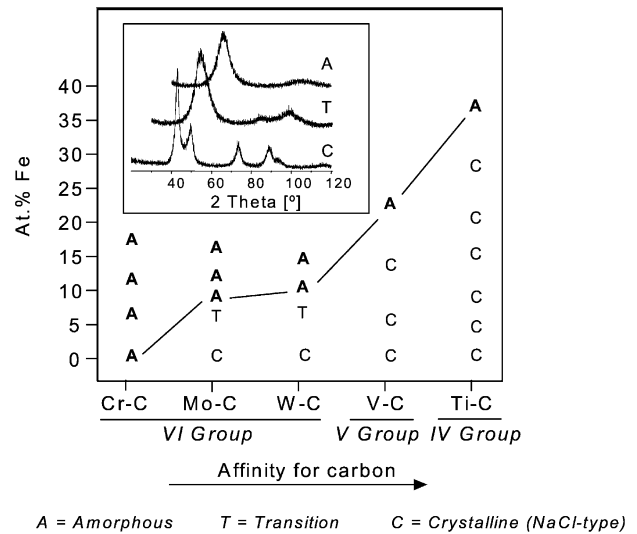


Fig. 8. Influence of Fe (Group VIII A) content on the transition crystalline → amorphous of M–M–C films; C=crystalline, T=mixed phases, A=amorphous.

M_1 –C system, where M =Ti, V and Mo, and M_1 =Fe (element of Group VIII). The binary systems exhibit NaCl-type f.c.c. structures. The addition of a third element from Group VIII, such as iron, leads to the occurrence of an amorphous structure with diffractograms of type II. The fraction of the doping element required for amorphization depends on the transition metal carbide, and is higher for stronger carbide formers. The crystalline → amorphous transition extends over a certain composition range, where gradual widening of the diffraction peaks occurs. A transition zone is clearly visible in the case of Mo–C-based systems, as it was in the W–C system. Concerning chromium carbide, the base structure is always amorphous and any addition of a third element does not contribute to change its spatial arrangement.

Structural analysis shows that the structure of W–M–C/N films does not depend on the preparation method of the targets from which they were sputtered.

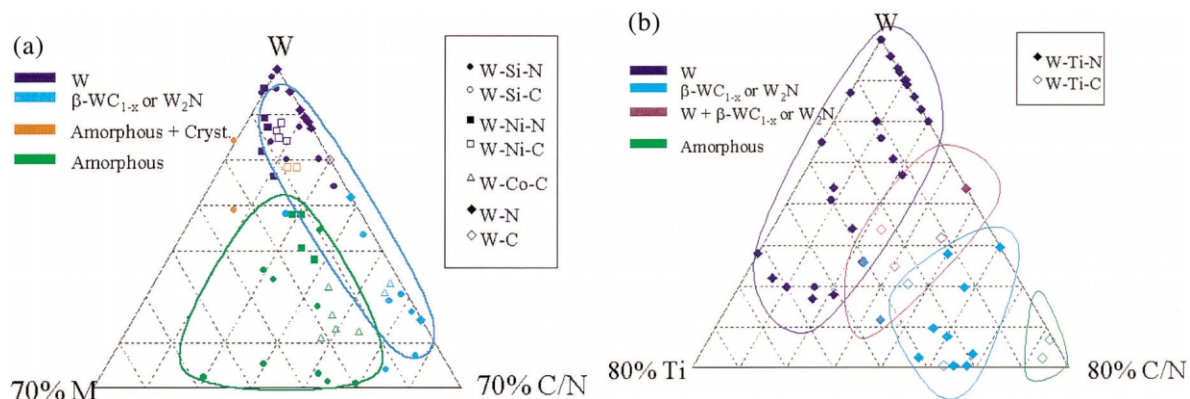


Fig. 7. Ternary diagrams of W–M/Si–C/N systems: (a) M =Fe, Co, Ni, Pd, Au and Si; and (b) M =Ti.

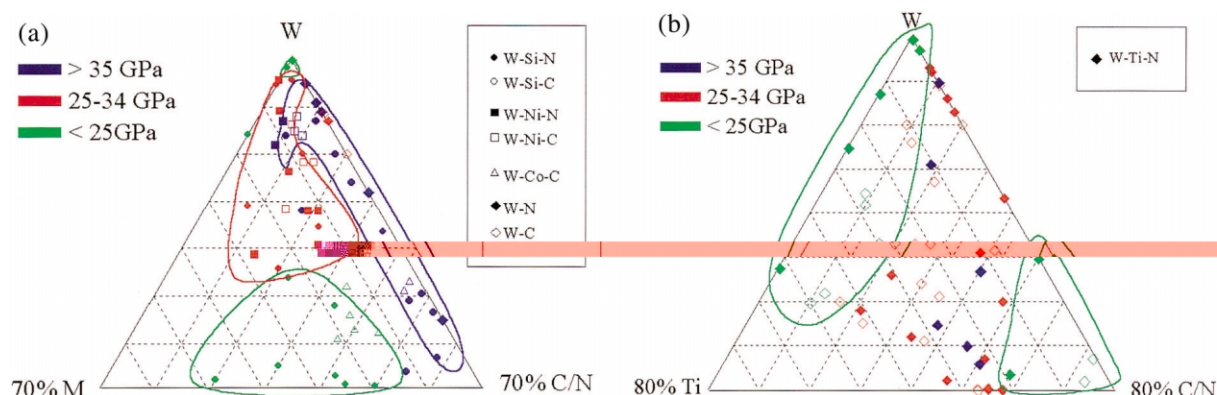


Fig. 9. Ternary diagram of W–M/Si–C/N chemical composition vs. hardness: (a) M=Co, Ni and Si; and (b) M=Ti.

Moreover, the degree of structural order in the film depends on the fraction of the admixed third element (Group VIII element or silicon). The systems are crystalline or amorphous, depending on the transition metal–carbon bond strength, and on the type and quantity of the admixed third element. If the doping element is a Group VIII element, all the carbides and nitrides studied are amorphous. The formation of amorphous phases seems to be related to the stability of the carbides or nitrides formed, which increases from Group VIII A to Group IV A of the Periodic Table. The incorporation of the third element modifies the degree of structural order in binary systems, and as the content of the third element increases, the film structure gradually evolves towards an amorphous state. The required quantity of the *amorphizing* element is higher as the carbide or nitride is more stable. The introduction of a third element changes the base metal/carbon bonding, this influence being more pronounced in films formed by carbides of metals close to Group VIII than of metals other than from Group VIII, i.e. Ti–C/N or V–C/N. In this case, higher quantities of the third element are necessary to bring about a transition to the amorphous phase.

3.3. Hardness

Two ternary diagrams (Fig. 9a,b) represent the hardness as a function of the thin film chemical composition. Fig. 9a shows the effect of the third element, which promotes a decrease in the structural order of W–C/N-based films. Fig. 9b shows the effect of titanium in the ternary system studied.

In the first case, the highest hardness is attained at the lowest concentration of the third element, which corresponds to the two structures: α -W and β -MC_{1–x} or β -W₂N (M=W, with elements in solid solution). The introduction of a non-metallic element into the tungsten lattice largely increases the hardness of the coatings. Some authors [29,33] have reached the conclusion that the increase in hardness of coatings with

tungsten and small amounts of carbon is due to uniform expansion of the α -W lattice. However, there is negligible change in the hardness as the atomic concentration of carbon or nitrogen exceeds a certain value. In solid solutions where the matrix is mainly W, an important increase in the hardness is attained up to approximately 8 at.% of carbon and 3 at.% of nitrogen. Further increase in the non-metallic fraction in the solid solution up to 18 at.% does not change the hardness. Rebholz et al. [30] obtained slightly higher hardness values for films with similar chemical compositions. The hardness decreases after reaching a maximum value, which was attributed to a change from isotropic to anisotropic lattice expansion.

In the W–Si–N system, the highest hardness values are also attained for low silicon content. An increase in silicon content induces a decrease in hardness. For W–Si (low N) films, there is good correlation between the increase in hardness and both the increase in lattice parameter and decrease in grain size. However, for films with higher nitrogen content, these trends are not systematically observed [39]. The homogeneity in the lattice distortion might be more adequate for understanding hardness variation. Generally, crystalline films exhibit higher hardness (35–41 GPa) than amorphous coatings (21–31 GPa).

The hardness of W–M (M=Fe, Ni, Co, Pd,...) solid solutions is higher than that of pure tungsten. For crystalline structures with high values of the (W+Me)/(C or N) ratio, it is possible to obtain phases with very high hardness values. For ratios in the range from 11 to 19, the hardness can reach 39 and 55 GPa for W–C and W–N, respectively. The metallic elements of Group VIII, when present in the film in a content which promotes the amorphous structure, give rise to the lowest values of hardness. However, amorphous structures where the tungsten content is higher in the chemical composition of the films show the highest hardness values in these kinds of structures. A decrease in Group

VIII element content in the film increases the hardness, due to the increase in covalent character of the atomic bonding, up to the limit where the crystalline structure is formed. It should be pointed out that a decrease in carbon/nitrogen content in the films might counteract the third element, driven by the formation of metastable phases with a lower degree of structural order.

A substitutional solid solution of titanium in tungsten (with or without low nitrogen content) exhibits the lowest hardness, similar to thin films with very high contents of a non-metallic element.



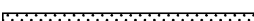

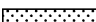

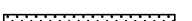








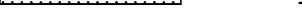
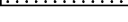
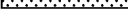


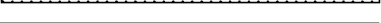
The hardness of ternary carbides and nitrides is a compromise between the hardening associated with distortion of the crystalline lattice due to the presence of third element in substitutional positions, and the soft-

ening or hardening due to a decrease in or enhancement of the covalent character of the carbide or nitride chemical bonding, which can be achieved by substitution of W with the third element. Finally, it should be noted that very high non-metallic element content can significantly decrease the material hardness.

3.4. Thermal behavior

The thermal evolution of W–C/N-based films is strongly dependent on their composition and structure. All studies were performed using three main techniques, XPS, DSC and EDXS, after each annealing. The structural evolution of W–Me/Si–C/N with increasing annealing temperature is summarized in Table 2.

Table 2
Structural stability of W–C/N-based systems

Composition	Structural stability with temperature
W ₅₆ C ₄₄	 $\beta\text{-WC}_{1-x} \xrightarrow{846^\circ\text{C}} \text{W}_2\text{C} + \text{WC}$
W ₄₆ N ₅₄	 $\text{W}_2\text{N} \xrightarrow{\approx 1050^\circ\text{C}} (\text{W})$
W ₅₂ Fe ₄ C ₄₄	 $\beta\text{-MC}_{1-x} \xrightarrow{856^\circ\text{C}} \text{M}_2\text{C} + \text{MC}$
W ₄₆ Fe ₁₃ C ₄₁	 $\text{A} \xrightarrow{758^\circ\text{C}} \text{M}_2\text{C}$
W ₄₂ Fe ₂₀ C ₃₈	 $\text{A} \xrightarrow{700^\circ\text{C}} \text{M}_2\text{C}$
W ₅₃ Co ₄ C ₄₃	 $\beta\text{-MC}_{1-x} \xrightarrow{856^\circ\text{C}} \text{M}_2\text{C} + \text{MC}$
W ₄₈ Co ₁₃ C ₃₉	 $\text{A} \xrightarrow{750^\circ\text{C}} \text{M}_2\text{C}$
W ₄₄ Co ₁₈ C ₃₈	 $\text{A} \xrightarrow{703^\circ\text{C}} \text{M}_2\text{C}$
W ₅₆ Ni ₄ C ₄₀	 $\beta\text{-MC}_{1-x} \xrightarrow{862^\circ\text{C}} \text{M}_2\text{C} + \text{MC}$
W ₅₁ Ni ₁₀ C ₃₉	 $\text{A} \xrightarrow{736^\circ\text{C}} \text{MC} + (\text{Ni})$
W ₄₇ Ni ₁₅ C ₃₈	 $\text{A} \xrightarrow{705^\circ\text{C}} \text{MC} + (\text{Ni})$
W–Ti–C	 $\beta\text{-MC}_{1-x} \xrightarrow{\approx 960^\circ\text{C}} \text{M}_2\text{C} + \text{MC}$
W ₄₂ Ti ₃₃ N ₂₅	 $\text{W}_2\text{N} / \text{TiN} + (\text{W})$ (no evolution) $\approx 1050^\circ\text{C}$
W ₆₉ Si ₃₁	 $\text{A} \xrightarrow{\approx 700^\circ\text{C}} \text{W}_5\text{Si}_3$
W ₄₁ Si ₄₁ N ₁₈	 $\text{A} \xrightarrow{\approx 750^\circ\text{C}} \text{W}_5\text{Si}_3$
W ₃₀ Si ₃₆ N ₃₄	 $\text{A} \xrightarrow{\approx 950^\circ\text{C}} (\text{W})$
W ₆₈ Si ₁₄ N ₁₈	 $\text{A} \xrightarrow{\approx 700^\circ\text{C}} (\text{W})$
W ₆₄ Si ₉ N ₂₇	 $\text{A} \xrightarrow{\approx 700^\circ\text{C}} (\text{W})$
W ₄₆ N ₅₄ *	 $\text{WN} \xrightarrow{\approx 1050^\circ\text{C}} \text{W}_2\text{N} + (\text{W})$
W ₃₅ Si ₁₅ N ₄₉ *	 $\text{W}_2\text{N} \xrightarrow{\approx 1050^\circ\text{C}} (\text{W})$
W ₂₇ Si ₂₀ N ₅₃ *	 $\text{A} \xrightarrow{\approx 1050^\circ\text{C}} \text{W}_2\text{N} + (\text{W})$

* Annealing in a N₂(H₂) atmosphere

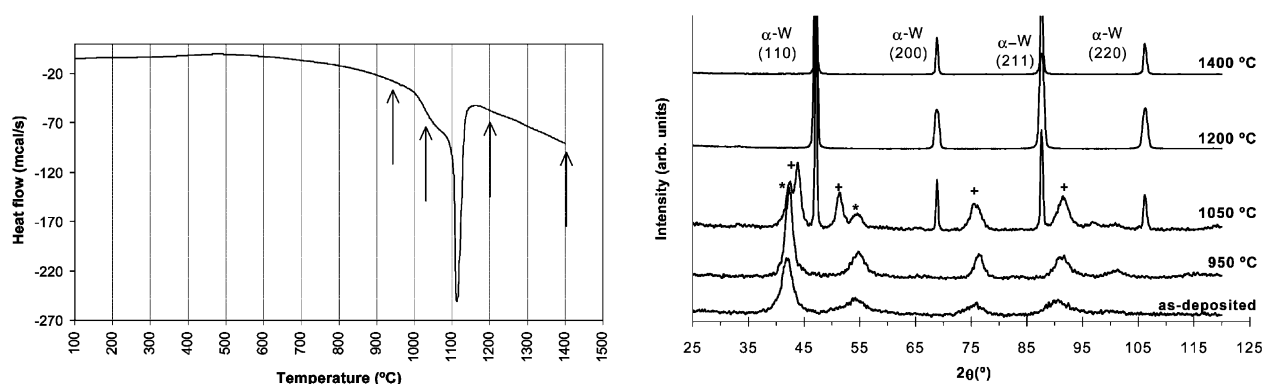


Fig. 10. Structural evolution of the W–N films with increasing temperature (+ = β -W₂N) monitored by DSC curve (left) and X-ray diffraction (right).

In order to evaluate the effects of the addition of a third element on the stability of the hard coating, the phase evolution of W–N/C-based films (without additions) with temperature was studied first. The structural behavior of W–C films without the addition of a doping element M is characterized by the formation of WC + W₂C from β -WC_{1-x} at 845 °C. Fig. 10 presents the structural evolution of W₄₆N₅₄ analyzed by the X-ray diffraction and DSC techniques. The DSC method allowed determination of the thermal cycle of annealing. In fact, two endothermic peaks were detected, close to the values of 1000 and 1100 °C. X-Ray diffraction identified the phases formed at these temperatures as α -W and β -W₂N, respectively. For temperatures equal to or higher than 1200 °C, the β -W₂N phase is no longer detected. All the systems studied tend to lose carbon and nitrogen if the annealing atmosphere is not enriched in these elements.

With regard to as-deposited W–M–C/N films, two different types of films have been studied: M = Group VIII of the Periodic Table and M = Ti. All films of the first type change structurally with annealing temperature. The resulting structures depend on the type of M and the metal content in the thin film. Iron and cobalt exhibit similar effects in the structural evolution of W–C/N-based films. In the course of annealing, the sequence of structural transformation with increasing temperature is: β -WC_{1-x}, β -W₂N or amorphous MC → M₂C/N → (M₆C/N) (this phase was only detected for some compositions [40]). In the case of M = Ni or Au, the Ni- and Au-rich terminal solid solutions are formed during the annealing. The higher the nickel or gold content in the film, the lower the temperature at which these solid solutions appear [38].

The addition of titanium or chromium to W–C/N systems stabilizes the as-deposited crystalline structure. In fact, no structural transformations of W–Ti–C/N or W–Cr–C/N were observed in successive annealing up to at least 960 °C. For example, X-ray diffractograms

of the W–Ti–N film (W₄₂Ti₃₃N₂₅) recorded after each annealing reveals thermal stability of the as-deposited phase up to the maximum temperature studied (1000 °C). Only a displacement of the (200) peak of β -W₂N/TiN to higher diffraction angles is observed as a function of increasing temperature. Such behavior can be attributed to two factors: a decrease in either the defect concentration or the amount of gaseous impurities in the film with temperature annealing, which leads to a decrease of interplanar distances, and an increase in compressive residual stress [32]. A slight increase in hardness has been observed with increasing annealing temperature up to 800 °C.

The decrease in hardness above an annealing temperature of 1000 °C is due to structural modifications of the substrate occurring during the heat treatment.

In W–Si-based films, two distinct behaviors as a function of nitrogen content can be observed. According to the results obtained by Reid et al. [35], the W–Si film begins to crystallize at 700 °C, with the formation of W₅Si₃ and W phases. The presence of nitrogen in W–Si-based coatings with Si content in the films higher than 15 at.% stabilizes the as-deposited structure. The W–Si–N film does not suffer appreciable changes with increasing temperature up to 1000 °C. The structure remains amorphous, and only some changes in the position and shape of the amorphous peaks were observed. Up to 900 °C, there are small shifts in the peak position to smaller diffraction angles with increasing temperature. However, the opposite is observed at temperatures higher than 900 °C. There is a significant shift to higher angles, associated with the change in shape of the peaks. In an analogous system (Mo–Si–N), Hirvonen et al. [41] attributed these phenomena to the relaxation and densification of the structure with temperature. In addition, for crystalline W–Si–N films (Si < 16 at.%), the presence of Si in the structure stabilized the β -W₂N nitride, which explains its detection at temperatures of 1200 °C, in contrast to the observation in films without silicon addition.

4. Conclusions

The W–M/Si–N/C sputter-deposited thin films have, as a function of chemical composition, a structure of solid solution (interstitial or substitutional) phases or transition metal carbides and nitrides, which allow some solubility of a third element without changing the structural order. However, the third element maximum content in the solid solution depends on the type of the solute. Thus, the structure of as-deposited films of W–M/Si–N/C and other Fe-doped carbides and nitrides of transition metals is characterized by a varying degree of structural order, depending on the film chemical composition. Beyond a certain fraction of a Group VIII transition metal, an amorphous phase appears. Such behavior might be attributed to two main causes: a dissimilarity of the atomic radius of the metallic matrix element and that of the solute, and a difference in the strength of W(M)–C/N and W(M)–third element chemical bonding. The first is mostly responsible for the *amorphizing* role of silicon in the W–Si–N system. The second can explain the difference in the structural order of the sputtered thin film containing palladium and gold; both elements have the same atomic radius, but only palladium induces the occurrence of amorphous structures in W–C/N-based films. Transition elements with strong carbon and nitrogen affinity and a small difference in atomic radius with respect to the matrix, such as Ti, inhibit the formation of amorphous phases. In certain cases, the doping of an amorphous film with Ti is sufficient to obtain a crystalline structure.

In general, crystalline films have greater hardness than amorphous ones. In W–M/Si–C/N (M=Co, Ni, Fe, Au,...) films, the highest hardness values are attained in films with low M or Si content. Except in films with low concentrations of C and N, which exhibit low hardness, for the systems examined in which a crystalline phase is always present (whatever the M content, such as W–Ti–C/N), the hardness is not greatly dependent on the film chemical composition.

The thermal stability of W–M/Si–C/N depends on the affinity of the third element for carbon or nitrogen. Among the several chemical compositions studied, only films containing a third element with strong or moderate affinity for C and N maintained their structure up to temperatures close to 1000 °C. Although the films formed by W–C/N and a weak or non-carbide-forming metal (Fe, Ni, Co, Pd, Au,...) showed various structural transformations, they tend to lose carbon and nitrogen if the annealing atmosphere is not enriched in these elements. With increasing annealing temperature, the thin films transform into the phases predicted by equilibrium phase diagrams.

On the basis of these results, it is possible to select an optimal composition of the film for the function

required. Generally, titanium, vanadium, chromium or silicon must be present in the chemical composition of transition-metal carbides and nitrides in order to stabilize the as-deposited structure, and make them usable in demanding applications.

References

- [1] R.A. Andrievski, J. Mater. Sci. 32 (1997) 4463.
- [2] B.M. Kramer, P.K. Judd, J. Vac. Sci. Technol. A 3 (6) (1985) 2439.
- [3] N.J. Archer, Tungsten carbide coatings on steel, Proceedings of the 5th International Conference on CVD, Buckingham, England, The Electrochem. Society, Princeton, 1975, p. 540.
- [4] P.K. Srivastava, T.V. Rao, V.D. Vankar, K.L. Chopra, J. Vac. Sci. Technol. A 2 (1984) 1261.
- [5] K. Fuchs, P. Rodhammer, E. Bertel, F.P. Nertzer, E. Gornik, Thin Solid Films 151 (1987) 383.
- [6] G. Keller, I. Barzen, R. Erz, W. Dotter, S. Ulrich, K. Jung, Fresenius, J. Anal. Chem. 341 (1991) 349.
- [7] A. Cavaleiro, M.T. Vieira, G. Lemperière, Thin Solid Films 197 (1991) 237.
- [8] Y. Pauleau, Rh. Gouy-Pailler, J. Mater. Res. 7 (8) (1992) 2070.
- [9] Y. Pauleau, Rh. Gouy-Pailler, S. Paidassi, Surf. Coat. Technol. 54/55 (1992) 324.
- [10] E. Quesnel, Y. Pauleau, P. Monge Cadet, M. Brun, Surf. Coat. Technol. 62 (1993) 474.
- [11] B. Trindade, M.T. Vieira, Thin Solid Films 252 (1994) 82.
- [12] P. Tagström, H. Högberg, U. Jansson, J.-O. Carlsson, J. Phys. IV 5 (1995) 967.
- [13] G. Auberger, R. David, 1st Colloquium International de Pulverisation Cathodique, CIP 73, Montpellier, Société Française du Vide, Paris, 1973, p. 275.
- [14] K.A. Taylor, Thin Solid Films 40 (1977) 189.
- [15] K. Fuchs, P. Rödhamer, E. Bertel, F.P. Netzer, E. Gornik, Vide Couches Minces 225 (Suppl. 2) (1987) 587.
- [16] R. Fella, H. Holleck, H. Shulz, Surf. Coat. Technol. 36 (1988) 257.
- [17] E. Eser, R.E. Ogilvie, J. Vac. Sci. Technol. 15 (2) (1978) 396.
- [18] E. Eser, R.E. Ogilvie, K.A. Taylor, Thin Solid Films 67 (1980) 265.
- [19] A. Cavaleiro, M.T. Vieira, G. Lemperière, Thin Solid Films 185 (1990) 199.
- [20] A. Cavaleiro, M.T. Vieira, G. Lemperière, Thin Solid Films 213 (1992) 6.
- [21] H.Y. Yang, X.-A. Zhao, J. Vac. Sci. Technol. A 4 (6) (1986) 1646.
- [22] P.K. Srivastava, V.D. Vankar, K.L. Chopra, 8(3) (1986) 379.
- [23] K. Machida, M. Enyo, I. Tosyoshima, Thin Solid Films 161 (1988) 191.
- [24] B. Trindade, M.T. Vieira, Thin Solid Films 206 (1991) 318.
- [25] A. Cavaleiro, B. Trindade, M.T. Vieira, Thin Solid Films 228 (1993) 80.
- [26] A. Cavaleiro, M.T. Vieira, J. Mater. Sci. 28 (1993) 6096.
- [27] B. Trindade, M.T. Vieira, E. Bauer Grosse, Surf. Coat. Technol. 75 (1995) 802.

- [28] A. Cavaleiro, B. Trindade, M.T. Vieira, *Surf. Coat. Technol* 60 (1993) 411.
- [29] J.M. Castanho, M.T. Vieira, *Surf. Coat. Technol* 102 (1998) 50.
- [30] C. Rebholz, J.M. Schneider, H. Ziegile, B. Rühl, A. Layland, A Matthews, *Vacuum* 49 (1998) 265.
- [31] A. Cavaleiro, B. Trindade, M.T. Vieira, *Surf. Coat. Technol.* 116–119 (1999) 944.
- [32] E. Le Patezour, A. Cavaleiro, *Mater. Sci. Forum*, in press.
- [33] P. Gouy-Pailler, Y. Pauleau, *J. Vac. Sci. Technol. A* 11 (1) (1993) 96.
- [34] A.G. Lahav, C.S. Wu, *J. Vac. Sci. Technol. B* 6 (1988) 1765.
- [35] J.S. Reid, E. Kolawa, R.P. Ruiz, M.A. Nicolet, *Thin Solid Films* 236 (1993) 319.
- [36] M.-L. Ger Vanishvili, R.B. Brown, *J. Mater. Res.* 10 (1995) 1710.
- [37] M.-L. Ger Vanishvili, Z.A. Munir, *J. Mater. Res.* 10 (1995) 2642.
- [38] B. Trindade, M.T. Vieira, E. Bauer Gross, *Acta Mater.* 46 (5) (1998) 1731.
- [39] C. Louro, A. Cavaleiro, *Vacuum*, in press.
- [40] B. Trindade, M.T. Vieira, E. Bauer-Grosse, *Acta Mater.* 46 (1998) 1731.
- [41] J.P. Hirvonen, et al., *Surf. Coat. Technol.* 6 (1988) 1765.